

lation was specific. A constitutively active recombinant human PAK1 phosphorylated p47^{phox} and MBP (11) in the absence of Rac-GTP, but did not stimulate phosphorylation of p67^{phox} (Fig. 5A). Modification of the NH₂-terminus of PAK may cause a conformational change that activates the kinase catalytic domain.

In vivo phosphorylation of p47^{phox} during neutrophil activation takes place on serine residues (Ser³⁰³, Ser³⁰⁴, Ser³²⁰, Ser³²⁸, Ser³⁴⁵, and Ser³⁴⁸) that are all located in a 14-kD COOH-terminal portion of the protein (12). p47^{phox} peptides containing all possible serine phosphorylation sites were tested in kinase assays (Fig. 5B). Substantial incorporation of ³²P was only observed with a single peptide containing Ser³²⁸. Additional control peptides such as the cyclic adenosine 3',5'-monophosphate-dependent protein kinase (PKA) substrate Kemptide or a protein kinase C (PKC) peptide substrate were not phosphorylated by PAK. A histone H4 peptide previously shown to be a substrate for an fMLP-stimulated neutrophil kinase (13) was phosphorylated to a similar extent as was the p47^{phox} peptide. These peptide data indicate that PAK phosphorylates a physiologically relevant site in p47^{phox}; this remains to be confirmed in vivo. The PAKs we have identified have many of the properties of a group of renaturable serine-threonine kinases that participate in NADPH oxidase activation (14), including inhibition of PAK activation by phosphatidylinositol 3-kinase inhibitors (11). We propose that we have identified the major 63- to 69-kD renaturable neutrophil kinases as PAK1 and PAK2.

We have established that a G protein-coupled receptor can regulate PAKs in mammalian cells. Our findings therefore support a link between the activation of heterotrimeric G proteins and the activity of Rac and related GTPases. Evidence from earlier studies indicates that Rac regulates the NADPH oxidase at the membrane level (15), and a direct interaction between Rac and p67^{phox} has been reported (16). The present work suggests that PAK-mediated phosphorylation events on p47^{phox} may play an important role in NADPH oxidase regulation.

REFERENCES AND NOTES

- G. M. Bokoch, *Trends Cell Biol.* **5**, 109 (1995); U. G. Knaus *et al.*, *Science* **254**, 1512 (1991); A. Abo *et al.*, *Nature* **353**, 668 (1991).
- G. M. Bokoch and A. G. Gilman, *Cell* **39**, 301 (1984); G. M. Bokoch, in *Current Topics in Membranes and Transport*, S. Grinstein and O. D. Rotstein, Eds. (Academic Press, San Diego, CA, 1991), vol. 35, pp. 65–101.
- G. M. Bokoch *et al.*, *J. Biol. Chem.* **269**, 31674 (1994).
- J. W. Voncken *et al.*, *Cell* **80**, 719 (1995).
- D. Rotrosen and T. L. Leto, *J. Biol. Chem.* **265**, 19910 (1990); W. M. Nauseef, R. D. Volpp, R. A. Clark, *Blood* **76**, 2622 (1990); P. G. Heyworth and J. A. Badwey, *J. Bioenerg. Biomembr.* **22**, 1 (1990); S. Dusi and F. Rossi, *Biochem. J.* **296**, 367 (1993).
- E. Leberer *et al.*, *EMBO J.* **11**, 4815 (1992); I. Herskowitz, *Cell* **80**, 187 (1995).
- E. Manser *et al.*, *Nature* **367**, 40 (1994).
- M. A. Sells *et al.*, in preparation; A. Polverino, M. Hutchison, M. Cobb, S. Marcus, in preparation.
- M. T. Quinn *et al.*, *J. Biol. Chem.* **268**, 20983 (1993); A. Abo *et al.*, *Biochem. J.* **298**, 585 (1994).
- X. Xu *et al.*, *J. Biol. Chem.* **269**, 23569 (1994).
- U. G. Knaus and G. M. Bokoch, unpublished observations.
- J. El Benna *et al.*, *J. Biol. Chem.* **269**, 23431 (1994).
- L. Liang and C.-K. Huang, *J. Leukocyte Biol.* **57**, 326 (1995).
- C. Huang and G. F. Laramée, *J. Biol. Chem.* **263**, 13144 (1988); S. Grinstein *et al.*, *ibid.* **268**, 20223 (1993); J. Ding and J. A. Badwey, *ibid.*, p. 17326; J. Ding *et al.*, *ibid.* **270**, 11684 (1995).
- O. Dorseuil, M. T. Quinn, G. M. Bokoch, *J. Leukocyte Biol.*, in press.
- D. Diekmann *et al.*, *Science* **265**, 531 (1994).
- Rac1 and RhoA proteins were cloned into pGEX-4T-3, expressed as GST fusion proteins in *E. coli*, and purified with the use of glutathione-Sepharose 4B beads (Pharmacia). The proteins were activated with GTP γ S at 500 nM free Mg²⁺ for 10 min at 30°C and washed with 5 mM MgCl₂-containing buffer. After incubation with cytosol, kinase activity was measured in 60 μ l of kinase buffer [50 mM Hepes (pH 7.5), 10 mM MgCl₂, 10 mM MnCl₂, and 0.2 mM dithiothreitol] containing 14 μ M [γ -³²P]ATP (10 Ci/mmol) for 20 min at 30°C. The reaction was stopped with SDS sample buffer, and results were visualized by SDS-polyacrylamide gel electrophoresis (PAGE) and autoradiography.
- E. Manser *et al.*, *J. Biol. Chem.* **267**, 16025 (1992).
- P. G. Heyworth *et al.*, *Mol. Biol. Cell* **4**, 261 (1993).
- Noncrossreactive antisera to PAK were raised in rabbits against purified GST (guanosine-S-triphosphate) fusion proteins representing amino acids 175 to 306 of rat p65^{pak} (PAK1) and amino acids 1 to 252 of rat PAK2 (8). Amino acid sequence comparison of rat with human PAK1 and PAK2 revealed 98 and 93% identity, which supports the observed cross-reactivity of these antisera with human neutrophil PAKs.
- Cells were lysed on ice in 50 mM Tris-HCl, 150 mM NaCl, 5 mM MgCl₂, 1 mM EGTA, 50 mM NaF, 10 mM sodium pyrophosphate, 1% NP-40, 2.5% glycerol, and 1 mM Na₃VO₄ (pH 7.5), containing the protease inhibitors phenylmethylsulfonyl fluoride, leupeptin, aprotinin, and pepstatin. Cells were then centrifuged for 10 min at 1000g. For immunoprecipitations, incubations with antibody (1:25) were for 2 hours at 4°C, followed by incubation with 60 μ l of 1:1 protein A beads for 60 min, then five 1.0 ml lysis buffer washes and two washes with kinase buffer. Kinase assays were as described in (17) but with 1.4 μ M [γ -³²P]ATP (100 Ci/mmol).
- P. Peveri, P. G. Heyworth, J. T. Curnutte, *Proc. Natl. Acad. Sci. U.S.A.* **89**, 2494 (1992).
- The full-length complementary DNA (cDNA) from human PAK1 (8) was cloned into pGEX-4T-3 for expression in *E. coli*. The protein was purified by glutathione-Sepharose affinity chromatography, eluted as the intact GST fusion protein, and assessed for kinase activity (17). Recombinant PAK1 was 80 to 90% pure as shown by Coomassie blue staining.
- I. Trilivas *et al.*, *J. Biol. Chem.* **266**, 8431 (1991).
- We thank C.-K. Huang for histone H4 peptide, M. Cobb and M. Hutchison for cDNA encoding the NH₂-terminal of rat PAK2, X. Xu for Rac2(D38A), B. P. Bohl for technical assistance, and A. Lestelle for editorial assistance. Supported by NIH grants P60 AR40770 and AI35947 (U.G.K.), HL48008 (G.M.B.), CA58836 (J.C.), M01 RR00833 (TSRI GCRC), and W. W. Smith Foundation grant C9201 (J.C.).

10 April 1995; accepted 31 May 1995

Peptide Binding and Presentation by Mouse CD1

A. Raúl Castaño,*† Shabnam Tangri, Jeffrey E. W. Miller, Hilda R. Holcombe, Michael R. Jackson,† William D. Huse, Mitchell Kronenberg, Per A. Peterson†

CD1 molecules are distantly related to the major histocompatibility complex (MHC) class I proteins. They are of unknown function. Screening random peptide phage display libraries with soluble empty mouse CD1 (mCD1) identified a peptide binding motif. It consists of three anchor positions occupied by aromatic or bulky hydrophobic amino acids. Equilibrium binding studies demonstrated that mCD1 binds peptides containing the appropriate motif with relatively high affinity. However, in contrast to classical MHC class I molecules, strong binding to mCD1 required relatively long peptides. Peptide-specific, mCD1-restricted T cell responses can be raised, which suggests that the findings are of immunological significance.

CD1 molecules are a heterogeneous family of proteins related to the classical MHC class I proteins both in overall sequence

A. R. Castaño, M. R. Jackson, P. A. Peterson, Scripps Research Institute, Department of Immunology, La Jolla, CA 92037, USA.

S. Tangri, H. R. Holcombe, M. Kronenberg, Department of Microbiology and Immunology and Molecular Biology Institute, University of California at Los Angeles, Los Angeles, CA 90095, USA.

J. E. W. Miller and W. D. Huse, Ixsys, San Diego, CA 92121, USA.

*To whom correspondence should be addressed. E-mail: castano@scripps.edu

†Present address: R. W. Johnson Pharmaceutical Research Institute at Scripps Research Institute, La Jolla, CA 92037, USA.

homology and by virtue of their association with β_2 -microglobulin (β_2 M) (1). However, they are as similar to MHC class II as to class I molecules in their α_2 domain, with little apparent similarity to either in the α_1 domain. CD1 molecules are expressed on antigen-presenting cells (2) and are recognized by selected T cells (3), but an antigen-presenting function for mCD1 (4) or its human equivalent hCD1d has not been reported. With less than 40% structural homology in the $\alpha_1\alpha_2$ domain to mCD1 (5), hCD1b can present nonpeptidic ligands (mycolic acids) derived from mycobacteria to T cells (6), but the structure of

the antigens bound to hCD1b and the nature of the proposed interaction has not been determined. To identify the possible peptide binding ability of mCD1, we produced recombinant soluble CD1-β₂M complexes in *Drosophila melanogaster* cells and used them to screen a random peptide phage display library (RPPDL). The absence of peptide-loading machinery in *D. melanogaster* cells results in the expression of class I molecules that are properly folded and functionally competent but essentially devoid of bound peptide (7). We and others have previously shown this approach to be useful in defining peptide binding motifs for classical and nonclassical MHC class I (8) and class II molecules (9).

Each clone of the RPPDL contained a random 22-amino acid sequence at the mature NH₂-terminus of the gene VIII protein (filamentous coat protein of the M13 bacteriophage). Recombinant soluble mCD1 was engineered with a COOH-terminal hemagglutinin (HA) tag, an epitope derived from the influenza HA protein (10, 11). In this way, mCD1-phage complexes could be identified with a HA tag-specific antibody. Forty-seven different clones were selected by mCD1 binding (Table 1). Alignment of the NH₂-terminal sequences encoded by these phages shows a well-defined core motif consisting of an aromatic Phe or Trp at position 1 (100% of the clones), an amino acid with a long aliphatic side chain (either Ile, Leu, or Met) at position 4 (80%), and a Trp at position 7 (75%). A large proportion (25 out of 47) of

the clones had either His or Asn at position 3. A minority of the clones did not fit this core motif. However, all of them could be aligned with an aromatic residue near the NH₂-terminus corresponding to position 1 of the core. Therefore, mCD1 seems to select phages with a hydrophobic binding motif, preferring aromatic residues at positions 1 and 7 and aliphatic residues in position 4,

with an overhanging NH₂-terminus.

To confirm the RPPDL data, we synthesized a peptide corresponding to the full-length, NH₂-terminal sequence of clone 99. Binding of ¹²⁵I-labeled p99 (see Table 2 for nomenclature) to mCD1 (12) was determined to be in the micromolar concentration range (Fig. 1A). The dissociation constant was calculated to be 0.9 μM by Scatchard analysis

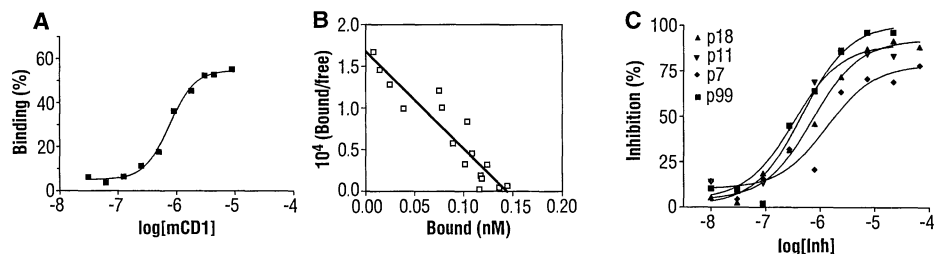


Fig. 1. Mouse CD1 binds specific peptides in solution. **(A)** ¹²⁵I-p99 binds to mCD1 in the micromolar range. **(B)** Scatchard analysis of ¹²⁵I-p99 binding to mCD1 shows a value for K_d of 9×10^{-7} M. Values for bound/free range from 0 to 0.0002. **(C)** Synthetic peptides corresponding to different sequences of selected phage clones bind to mCD1 as tested by a competitive binding assay. Curves represent the percent of inhibition of ¹²⁵I-p99 binding to mCD1 versus the logarithm of the molar concentration of inhibitor peptide (Inh) and were fitted by nonlinear regression analysis to a sigmoidal function.

Table 1. Mouse CD1-binding motif determined by screening RPPDL (10, 26). The alignment of the sequences of the different mCD1-specific phage clones shows a binding motif in positions 1, 4, and 7. Amino acids specific to the motif are shown in boldface. An unbiased representation of the sequences obtained (one out of two) is shown.

Phage	Amino acid sequence
	1 4 7
99	YEHDFHHIREWGNHWKNFLAVM
36	EFSLFKDIYRWGNWAAAGFYGV
24	SFCLPDSIFDWGARGAEWHVG
1	SCNMWRNIYSWGATFPQDHIF
20	DMDLFQHLSCWGTDFADMMFDE
101	SCAWFLHLRQWGNNSNWTYIFGV
30	MHFGWYHLSEWGIKLAALIGFEM
54	ETGWFHNLTAWCEESVYALHIM
52	SPGLFDNLKTWGTREHFMFSL
18	YEKPWQNLWDWGAEAFKDLLDK
7	ELWRNLRRLWGYCMNLSNMPL
11	LSPDWSELRLRWGTWAAAEVFEL
39	QSFMMRWGQEFHNMILNV
83	TALGWVHHEWGEESKFPWGN
76	QDYWTNMLIWGSMLLWLSLFGADP
15	HDYWQSMNHWGGVYGGCVPMCK
16	YEEMWQVFKAGQEWVPSYFPM
C4	QIPFQIQAYLWVCCQEVTDLL
69	IDQMWWQDPRWGXEEIDHD
84	SAFEYIQLTVSGWLPPLMLGLF
92	EKFEILCINYGWISDLCEAIA
3	WHDEDVLFRLNGEATLWLAEY
59	DWECMYDFPCWRGXCVLNSTG
22	DQTYKFEYNMGKDVTSLVICYW
34	DNWIDSLVICVGTGYSGLAAY
	W L W
	F I
	M

Table 2. Structural requirements for peptide binding to mCD1 (26). Dissociation constants (molar) for unlabeled peptides were determined from the molar concentration giving 50% inhibition of ¹²⁵I-p99 binding to mCD1 in a competitive binding assay (12, 27). The ratio relative to p99 is shown. Synthetic peptides were named corresponding to the selected clone from the phage library. Position 1 is the first anchor position; amino acids NH₂-terminal to this position were assigned negative numbers. Peptide sequences of the p99a series correspond to a variant phage clone derived from phage 99 (8) and show fivefold higher affinity than their p99 counterparts. NB, nonbinder, defined as those peptides that show no significant inhibition at a 200 μM concentration.

Peptide	Sequence	K_d	Ratio
	1 4 7		
p7	ELWRNLRRLWGYCMNLSNMPL	$(9.3 \pm 1.3) \times 10^{-7}$	6
p11	LSPDWSELRLRWGTWAAAEVFEL	$(1.5 \pm 0.4) \times 10^{-7}$	1
p18	YEKPWQNLWDWGAEAFKDLLID	$(2.4 \pm 0.8) \times 10^{-7}$	2
p99	YEHDFHHIREWGNHWKNFLAVM	$(1.5 \pm 0.3) \times 10^{-7}$	1
	-4 1 7 20		
p99.-4.20	YEHDFHHIREWGNHWKNFLAVMGG	$(1.7 \pm 0.3) \times 10^{-7}$	1
p99	Y-----M	$(1.5 \pm 0.3) \times 10^{-7}$	1
p99.-4.16	Y-----A	$(7.8 \pm 2.8) \times 10^{-7}$	5
p99.-4.14	Y-----F	$(2.1 \pm 0.3) \times 10^{-6}$	14
p99.-4.12	Y-----K	$(5.8 \pm 1.8) \times 10^{-6}$	39
p99.-4.10	Y-----H	$(1.1 \pm 0.4) \times 10^{-4}$	710
p99.-4.8	Y-----G	NB	
	H-----G	$(2.5 \pm 0.1) \times 10^{-7}$	2
p99.-2.20	H-----G	$(6.3 \pm 1.5) \times 10^{-7}$	4
p99.1.20	F-----G	NB	
p99.3.20	H-----G	NB	
p99.5.20	R-----G	NB	
p99.-2.15	H-----L	$(4 \pm 0.1) \times 10^{-7}$	3
p99.1.12	F-----K	$(2.6 \pm 0.5) \times 10^{-5}$	175
p99.1.7	F-----W	NB	
	AHEH-----K	$(1.1 \pm 0.2) \times 10^{-6}$	8
p99a.-4.12	AHEH-----K	$(1.1 \pm 0.2) \times 10^{-6}$	8
p99a.-2.15	EH-----L	$(1.1 \pm 0.1) \times 10^{-7}$	1
p99a	EH-----K	$(8.6 \pm 2) \times 10^{-7}$	6
p99a.-2.8	EH-----G	$(3.9 \pm 0.7) \times 10^{-5}$	260
	-4 1 7 18		
p99.A1	Y--A-----M	$(2 \pm 1) \times 10^{-4}$	1300
p99.A2	Y--A-----M	$(1.5 \pm 0.5) \times 10^{-7}$	1
p99.A3	Y--A-----M	$(3.9 \pm 1.3) \times 10^{-7}$	3
p99.A4	Y--A-----M	$(5.8 \pm 1.1) \times 10^{-5}$	380
p99.A7	Y--A-----M	$(3.6 \pm 0.7) \times 10^{-5}$	240
p99.A1,A7	Y--A--A-----M	$(7.5 \pm 1.9) \times 10^{-6}$	50
p99.A8	Y--A-----M	$(2.1 \pm 0.4) \times 10^{-7}$	1
p99.A11	Y--A-----M	$(7.0 \pm 0.9) \times 10^{-7}$	5
p99.A14	Y--A-----M	$(2.7 \pm 0.6) \times 10^{-7}$	2

(Fig. 1B), with fast association-dissociation kinetics (13). No binding to CD1 was detected in the same concentration range of a shorter version ^{125}I -p99.-4.10 (which lacked the eight COOH-terminal amino acid residues), suggesting that mCD1 preferentially binds longer peptides. Three additional sequences, which contained the motif but were otherwise quite different from p99, were selected from the RPPDL. All three peptides tested, corresponding to the full-length, NH₂-terminal 20- to 22-mer sequences of phage clones 7, 11, and 18, showed binding to mCD1 (Fig. 1C), and the dissociation constants were similar to that for p99 (1.5×10^{-7} M) (Table 2).

The data presented suggest that CD1 binds peptides with extended NH₂- and COOH-termini flanking the core binding motif. To further characterize the requirements for binding, we synthesized versions of the p99 peptide truncated at either the NH₂-, the COOH-terminus, or both. Their binding affinities were determined as above. Progressive truncations at the COOH-terminus resulted in a steady decrease of affinity, an approximately one-half reduction per residue (Table 2). Further COOH-terminal truncations near the core binding motif significantly affected the ability of the peptide to bind mCD1 (Table 2, p99.-4.12 versus p99.-4.10). The situation was similar at the NH₂-terminus of the peptide, where elimination of the four amino acids preced-

ing the core motif resulted in a one-fourth reduction in the binding affinity. However, if further NH₂-terminal truncations were made beyond the first anchor residue Phe¹, binding of these peptides to mCD1 could not be detected. A peptide derived from p99 with truncations at both the COOH- and NH₂-termini (p99.-2.15) bound with higher affinity than that predicted from the above experiments, suggesting that optimal peptide lengths might be important for maximal binding affinity. We conclude that peptide binding by mCD1 exhibits characteristics similar to those for class II peptide interactions (14).

The importance of the motif for peptide binding was tested by substitutions of the proposed anchor residues with Ala. Substitution of anchor Phe¹ with Ala resulted in a decrease in the ability of the peptide to bind mCD1 [dissociation constant (K_d) for p99.A1 was $\sim 2 \times 10^{-4}$ M] (Table 2). Ala substitution of anchor Ile⁴ reduced the affinity by a factor of 380 and of Trp⁷ by a factor of 240. In contrast, substitution of His³ did not alter the binding affinity, demonstrating that position 3 is probably not an anchor. Surprisingly, double Ala substitutions at positions 1 and 7 produced an unexpected, heterocyclic, compensatory effect, such that binding was reduced only by a factor of 50. Ala substitutions at locations other than the anchor positions had rela-

tively little effect on peptide binding, confirming the importance of the motif we have identified. Because of a bias in the construction of the RPPDL, Gly occurred frequently at position 8 and is unlikely to be part of the motif. Indeed, Ala substitution at this position did not affect the binding affinity (Table 2), and nonconservative substitutions are tolerated in this position (Table 1) (8). The replacement of other aromatic amino acids (Trp¹¹ and Phe¹⁴) with Ala exerted only a minor influence, demonstrating that the presence of the motif is the critical component, rather than the overall hydrophobic character, in determining the affinity of a peptide for mCD1.

To assess the immunological relevance of the CD1-peptide complexes, we raised T cell lines. This was done by immunizing mice with mouse RMA-S cells transfected with mCD1 (15) that had been incubated with the mCD1-binding peptides p99a, p99a.-2.15, or p99 (16). T cell lines were isolated from lymph node-derived cells. The experiments shown below were done with a line raised to peptide p99a.

Cytotoxic T cells recognized CD1⁺ RMA-S transfectants in the presence of the immunizing peptide but not if the peptide was omitted (Fig. 2A); likewise, RMA-S transfectants expressing the thymus leukemia antigen (TL⁺ RMA-S) incubated with the peptide were not recognized. Three different mCD1⁺ transfectants—RMA-S T cells (H-2^b), L cell fibroblasts (H-2^k), and J774 macrophages (H-2^d) (17)—stimulated the T cells but only in the presence of the specific peptide. The mCD1-restricted cytotoxic T lymphocyte (CTL) activity was partially blocked (65% inhibition) by R377 [a rabbit antiserum specific for mCD1 (18)] (Fig. 2B), probably a reflection of its polyclonality. The control, pre-bleed serum from the same rabbit did not block CTL effector activity nor did a monoclonal antibody (mAb) specific for K^bD^b or a control immunoglobulin G (IgG) rat antiserum. These results demonstrate an absolute requirement for both p99a and CD1 by the CTLs and independence of any other MHC molecules. Peptide specificity was tested with two additional mCD1-binding peptides. CD1⁺ RMA-S transfectants incubated with p11 and p18 were weakly or not recognized at all (Fig. 2C). Furthermore, both peptides blocked the recognition of the reference p99a in a peptide inhibition assay (Fig. 2D). These data argue against conventional CTL recognition of a conformational change of mCD1 upon peptide binding. Rather, they suggest a more conventional model in which some amino acid side chains, such as the anchor motif, contribute to mCD1 binding and others to T cell receptor (TCR) recognition.

To test the importance of the anchor

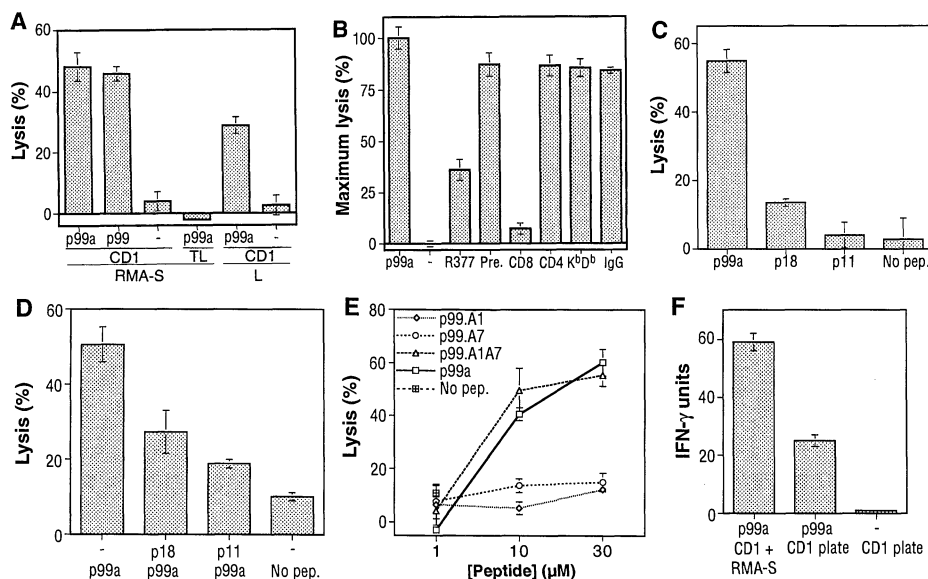


Fig. 2. Peptide-specific recognition of mCD1⁺ target cells by cytotoxic T cells. (A) Lysis of CD1⁺ RMA-S and CD1⁺ L target cells incubated with or without (–) peptide p99a and TL⁺ (T18d) RMA-S with p99a. (B) Antibody inhibition of CTL lysis of CD1⁺ RMA-S targets loaded with p99a (16). The percentage of maximum lysis is shown, relative to the value in the presence of p99a alone. Pre., pre-bleed serum. (C) Specific peptide sequences are required for mCD1-restricted lysis. Shown is the lysis of mCD1⁺ RMA-S cells pulsed with 10 μM p99a, 30 μM p11, or 30 μM p18. No pep., no peptide. (D) Peptide inhibition of lysis by preincubation of mCD1⁺ RMA-S cells with peptides p11 or p18 (30 μM) followed by pulsing with p99a (10 μM). (E) Peptide anchor amino acids are important for mCD1-restricted recognition. We tested mCD1⁺ RMA-S targets pulsed with the Ala-substituted peptides indicated. (F) Interferon γ (IFN- γ) produced by T cells when stimulated with plate-bound mCD1 in the presence or absence of p99a or with CD1⁺ RMA-S cells pulsed with p99a, measured as units determined by enzyme-linked immunosorbent assay (28).

residues in antigen recognition, we analyzed Ala mutants of p99 at anchor positions. The full-length peptide p99 elicited a lytic activity similar to that of the immunizing p99a (Fig. 2A). Ala-substituted peptides p99.A1 and p99.A7, with highly impaired binding capacity to mCD1, did not stimulate a cytotoxic response (Fig. 2E). However, the double Ala-substituted peptide p99.A1A7 was recognized, in concordance with its higher affinity. In summary, the ability of a synthetic peptide to bind to soluble mCD1 correlated with its ability to stimulate mCD1-restricted T cells in vitro.

In a cell-free system, soluble mCD1 bound to plates (19) was effective in stimulating the T cell line but only in the presence of peptide (Fig. 2F). Furthermore, no difference in killing activity was detected when peptide loading and CTL assays were done in serum-free medium (17). These experiments suggest that processing of the 14-mer p99a is not required for T cell recognition and confirm that mCD1 is the antigen-presenting molecule.

The origin and diversity of mCD1-reactive T cells is unknown. Fluorescence-activated cell sorting analysis indicated that 90% of the cells were $\alpha\beta\text{TCR}^+$ with no detectable $\gamma\delta$ population (17). Ninety percent of the cells were $\text{CD8}\alpha\beta^+\text{CD4}^-$. Consistent with this, CTL lysis was able to be inhibited by CD8 mAbs, but not with CD4 mAbs (Fig. 2B). The mCD1-restricted CTLs, therefore, had a conventional phenotype for class I-reactive cells from lymph node. However, mCD1 has recently been shown to positively select and react with a set of CD8^- T cells with an invariant $\text{TCR}\alpha$ chain (20), suggesting that at least two populations of mCD1-reactive T cells may exist.

The features of the mCD1-peptide interaction we describe closely match the characteristics of peptide interactions with MHC class II peptides. Similar to class II peptides, mCD1 prefers long peptides (14, 21) with hydrophobic and bulky amino acids at specific positions (9), and the affinity of the interaction is similar to that of naturally processed peptides co-purified with class II molecules ($K_d = 0.1 \times 10^{-7}$ to 2.3×10^{-7} M) (14). However, the mCD1 motif has three highly restricted anchors, mutations of which greatly reduce peptide binding, a feature that more closely resembles class I-peptide interactions (22). Mouse CD1 has a preference for peptides with hydrophobic residues, a feature shared by the molecular chaperone BiP and HMT-M3 (8, 23, 24). However, BiP presents a generalized requirement for large hydrophobic residues at alternating positions with little specificity for particular amino acids. These common features suggest that a hydrophobic groove may be the basic opera-

tional structure for ligand binding by MHC-related proteins, where specificity is achieved by pockets with chemical and structural complementarity for the ligands. In contrast to our findings with mCD1, hCD1b has been shown to present processed mycolic acids to T cells (6). These differences suggest that the various members of the heterogeneous CD1 family may have diverse functions that evolved for specific tasks, perhaps dedicated to the presentation of antigens from a limited subset of pathogens. We cannot exclude that altered peptides, for example modified with lipids, are the natural ligands for mCD1; however, the fact that mCD1 binds unmodified synthetic peptides with a reasonable affinity clearly differentiates it from HMT-M3 (24). Although our data do not exclude alternative functions for mCD1—for example, as a ligand for intact or denatured proteins in specific cellular compartments—they support the idea that mCD1 is an antigen-presenting molecule that presents a unique set of peptides to T cells.

REFERENCES AND NOTES

1. F. Calabi and C. Milstein, *Nature* **323**, 540 (1986); C. Terhorst *et al.*, *Cell* **23**, 771 (1981).
2. F. Sallusto and A. Lanzavecchia, *J. Exp. Med.* **179**, 1109 (1994); E. Fithian *et al.*, *Proc. Natl. Acad. Sci. U.S.A.* **78**, 2541 (1981); M. Van de Rijn *et al.*, *Hum. Immunol.* **9**, 201 (1984).
3. S. Porcelli *et al.*, *Nature* **341**, 447 (1989); S. P. Balk *et al.*, *Science* **253**, 1411 (1991).
4. S. P. Balk, P. A. Bleicher, C. Terhorst, *J. Immunol.* **146**, 768 (1991); A. Bradbury, K. T. Belt, T. M. Neri, C. Milstein, F. Calabi, *EMBO J.* **7**, 3081 (1988).
5. F. Calabi, J. M. Jarvis, L. Martin, C. Milstein, *Eur. J. Immunol.* **19**, 285 (1989).
6. E. M. Beckman *et al.*, *Nature* **372**, 691 (1994); S. Porcelli, C. T. Morita, M. B. Brenner, *ibid.* **360**, 593 (1992).
7. M. R. Jackson, E. S. Song, Y. Yang, P. A. Peterson, *Proc. Natl. Acad. Sci. U.S.A.* **89**, 12117 (1992).
8. J. E. W. Miller *et al.*, unpublished results.
9. J. Hammer, B. Takacs, F. Sinigaglia, *J. Exp. Med.* **176**, 1007 (1992); J. Hammer *et al.*, *Cell* **74**, 197 (1993).
10. Oligonucleotides and the polymerase chain reaction were used to engineer a mCD1.1 complementary DNA (4) encoding the extracellular domains followed by a HA epitope (YPYDVPDYAS) (26) and a His₆ tag. This construct was cloned into a pRMHa-3 vector and cotransfected with a murine $\beta_2\text{M}$ -pRMHa-3 construct into *D. melanogaster* SC2⁺ cells. Stable transfectants were established as described (7), and secreted CD1- $\beta_2\text{M}$ complexes (mCD1) were isolated by affinity chromatography with a Ni-NTA column (Qiagen) and purified by fast protein liquid chromatography with a Mono Q column (Pharmacia) (11). A codon-based RPPDL consisting of a 22-amino acid random peptide with a Gly residue at position 12, expressed at the NH₂-terminus of gene VIII protein of the M13 bacteriophage, just after the leader peptide, was screened with mCD1. Phage clones that bind mCD1-specific clones were revealed with alkaline phosphatase-conjugated mAb 7F11 (Biosite) to the HA epitope, plaque-purified, and sequenced (8).
11. Y. Sykulev *et al.*, *Immunity* **1**, 15 (1994).
12. Synthetic peptides were purified by high-performance liquid chromatography and their identity confirmed by mass spectrometry and quantitative amino acid analysis. The p99 peptide was radiiodinated by the lactoperoxidase method (25). Labeled peptide was purified with a PepRPC (Pharmacia) C₁₈ reversed-phase column. Radioactive fractions were lyophilized and

resuspended in 1% bovine serum albumin in phosphate-buffered saline (PBS) and stored at -20°C . The concentration of mCD1- $\beta_2\text{M}$ in PBS was determined by protein assay (Bio-Rad). For peptide binding and Scatchard analysis, various concentrations of purified mCD1 were mixed with 20,000 cpm of ¹²⁵I-p99 (~220 pM) in 50 μl of PBS. After incubation at room temperature for 2 hours, mCD1-peptide complexes were separated from free peptides by gel filtration (Bio-Gel P-30, Bio-Rad). For competitive inhibition assays, unlabeled peptides and 20,000 cpm of ¹²⁵I-p99 were incubated with 2 μM CD1.

13. A. R. Castaño, unpublished results.
14. A. Y. Rudensky, P. Preston-Hurlburt, S.-C. Hong, A. Barlow, C. A. Janeway Jr., *Nature* **353**, 622 (1991); R. M. Chiczy *et al.*, *ibid.* **358**, 764 (1992); D. F. Hunt *et al.*, *Science* **256**, 1817 (1992).
15. M. Teitell *et al.*, unpublished results.
16. C57BL/6 mice were immunized intramuscularly with 10^7 CD1⁺ RMA-S cells preloaded with 10 μM peptide along with 10 μM peptide in adjuvant given in the contralateral thigh and boosted 1 week later. Lymph node cells were harvested 7 days later, stimulated in vitro with irradiated mCD1⁺ RMA-S cells prepulsed with peptide, and restimulated weekly in the presence of interleukin-2 (10 U/ml). For CTL assays, effector cells were incubated with ⁵¹Cr-labeled target cells [at an effector/target ratio (E/T) of 50:1] pulsed with peptide (10 μM unless otherwise indicated) or no peptide. Antibodies to CD8 α , CD8 β , CD4, K^DD^B (28-8-6s), or control TL rat IgG mAb HD168 (PharMingen) were used for blocking assays (at 10 μg /well) or in fluorescence-activated cell sorting. Rabbit antibody R377 to mCD1 and the pre-bleed antiserum were used at a 1:20 dilution. For serum-free medium studies, HL1 (Ventrex) was used in place of RPMI plus fetal calf serum. In peptide-blocking experiments, mCD1⁺ RMA-S target cells were preincubated with 30 μM blocking peptide for 1 hour at 37°C, washed extensively, and then incubated with 10 μM p99a.
17. S. Tangri, unpublished results.
18. R377 antiserum to mCD1 was raised by injecting rabbits with 200 μg of mCD1 in Freund's complete adjuvant followed by three injections with 100 μg in Freund's incomplete adjuvant. The antiserum specificity was tested by immunoprecipitation and immunofluorescence.
19. Plates (96-well, flat-bottom) were coated with 7F11 mAb (5 μg /ml), extensively washed, and incubated with mCD1 (3 μg /ml) overnight. The plates were then washed, and the relevant peptide, or a no-peptide control, were added and incubated for 2 hours at 37°C. We then added 10^4 CTL effectors per well and harvested supernatants after 48 hours and analyzed them in an interferon γ enzyme-linked immunosorbent assay.
20. A. Bendelac *et al.*, *Science* **268**, 863 (1995).
21. L. J. Stern *et al.*, *Nature* **368**, 215 (1994).
22. M. L. Fahnestock *et al.*, *Biochemistry* **33**, 8149 (1994); Y. Saito, P. A. Peterson, M. Matsumura, *J. Biol. Chem.* **268**, 21309 (1993).
23. S. Blond-Elguindi *et al.*, *Cell* **75**, 717 (1993).
24. C.-R. Wang *et al.*, *ibid.*, in press; S. M. Shawar, J. M. Vyas, J. R. Rodgers, R. G. Cook, R. R. Rich, *J. Exp. Med.* **174**, 941 (1991).
25. E. Harbow and D. Lane, in *Antibodies: A Laboratory Manual* (Cold Spring Harbor Laboratory, Cold Spring Harbor, NY, 1988), p. 336.
26. Abbreviations for the amino acid residues are: A, Ala; C, Cys; D, Asp; E, Glu; F, Phe; G, Gly; H, His; I, Ile; K, Lys; L, Leu; M, Met; N, Asn; P, Pro; Q, Gln; R, Arg; S, Ser; T, Thr; V, Val; W, Trp; and Y, Tyr.
27. R. Muller, *Methods Enzymol.* **92**, 589 (1983).
28. T. A. T. Fang and T. R. Mosmann, *J. Immunol.* **144**, 1744 (1990).
29. Supported by grants from NIH (P.A.P., M.K., H.R.H.), the Ministerio de Educacion y Ciencia of Spain (A.R.C.), and the Jonsson Cancer Center and the Jaye Haddad/Concern Foundation (S.T.). The technical assistance of the peptide and DNA facilities of the Scripps Research Institute and Robert Wood Johnson Pharmaceutical Research Institute is gratefully acknowledged.

17 March 1995; accepted 12 June 1995